

University of Szeged
Department of Applied Informatics

Novel MR Image Analysis Strategies: Applications in Multiple Sclerosis

Summary of the Doctoral Thesis

by

László G. Nyúl

Thesis advisors:

Jayaram K. Udupa, PhD and **Attila Kuba, PhD**

Szeged
2002

1 Introduction

This thesis deals with issues from different aspects of medical image processing—image segmentation (Chapters 3 and 4), image registration (Chapter 5), and image analysis (Chapter 6). Chapter 2 describes a preprocessing procedure that facilitates both image segmentation and analysis. Although the techniques and algorithms are described within the context of an actively pursued application, namely the analysis of brain MRI in Multiple Sclerosis, most of the methods described here are applicable to other brain diseases and other modalities as well. They even have potential in non-medical applications.

2 Standardization of the MRI Intensity Scale

Magnetic Resonance Imaging (MRI) has revolutionized radiological imaging of the internal structures of the human body. It has the advantage of being noninvasive with no known health hazards. A variety of MRI protocols are currently available, with and without the use of contrast agents. These protocols allow the setting up of different contrasts among the different tissues within the same organ system. A major difficulty with the MRI techniques, however, for most protocols has been that image intensities do not have a fixed meaning, even within the same protocol, for the same body region, for images obtained on the same scanner, for the same patient.

We recently developed an image processing method for MRI intensity standardization wherein all images (independent of patients and the specific brand of the MR scanner used) can be transformed in such a way that for the same protocol and body region, in the transformed images similar intensities will have similar tissue meaning. The method was published in [17, 18, 19, 22, 26] and is described and extensively evaluated in Chapter 2 of the thesis.

The main idea underlying the methods is to deform the image histograms using certain landmarks so that they match a mean histogram determined through training. In the original method [19], we utilized a low and a high percentile point together with the mode corresponding to the foreground in the image as the landmarks. Although, for display, this achieves a remarkably consistent window level and width setting, for image segmentation, the mode-based matching is often too sensitive to the actual location of the mode which is often quite variable. In a later work [26], we described variants of the method that utilized other landmarks, the quartiles and deciles, in particular the median corresponding to the foreground in the image, in addition to the low and high percentiles, to overcome the difficulties with the mode. The method is easy to implement and rapid in execution. The actual transformation itself can be stored as a lookup table in the image header. The transformed images permit predetermined display window settings and also facilitate image segmentation. Figure 1 shows image examples and their histograms before and after standardization.

The method consists of two steps. In the first (“training”) step, a set of images of the same body region and protocol corresponding to a population of patients is given as input. The parameters of a histogram transformation are “learnt” from these image data and a few additional input parameters are determined. These additional parameters may vary and are used to fine tune the transformation to the protocol, the body region, and possibly the application that will work on the transformed data. This step needs to be executed only once for a given protocol and for a given body region. In the second (“transformation”) step, the images are transformed using the parameters learnt in the first step. This transformation is

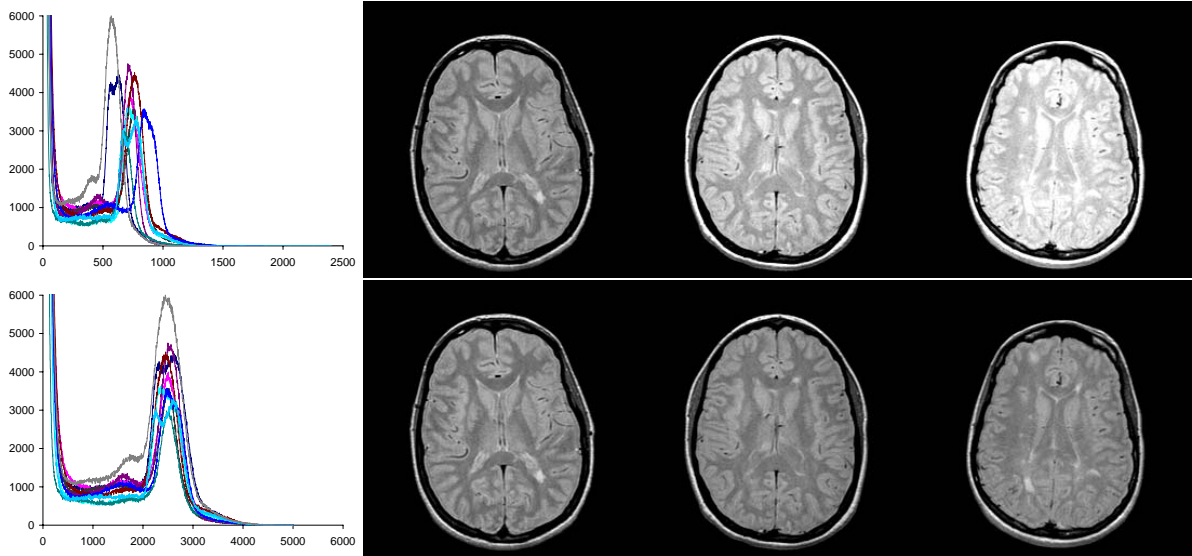


Figure 1: Histograms of 10 different brain images obtained using identical PD protocols on the same scanner and center slices from 3 of those datasets (top row). Histograms of the same images after after standardization, and the corresponding slices from the standardized images (bottom row). The images are displayed at fixed gray level windows.

image dependent and needs to be done for each given image.

Although once the training step is done the corresponding transformation step is fully determined, there are several possibilities to tailor the standardizer to the specific needs of an application. We delineated a theory and established a set of theorems for the mode-based configuration that are crucial to guarantee the correct behavior (i.e., preserving the intensity relations between voxels) of the standardizer for any given image. The theory readily generalizes to other percentile-based configurations.

3 Image Segmentation

In brain MRI analysis, usually the first step is to segment the brain parenchyma and remove the extrameningeal tissues and bone. Also, in many situations, separating the gray matter and white matter is desirable, as well as separating normal and abnormal tissues such as normal appearing and abnormal normal appearing white matter, and lesions.

Image segmentation techniques using fuzzy connectedness principles [35] have been used successfully in several large applications in recent years: MR brain image analysis for quantifying white matter lesions and brain tumors, segmentation of vessel structures and artery-vein separation in MRA, craniofacial muscle segmentation, and mammographic fibroglandular density quantification. However, there were several parts in these techniques where improvements can be achieved. When the fuzzy connectedness algorithms were first introduced they could not be used for interactive processing due to their excessive computational requirements.

In an attempt to substantially speed up the fuzzy connectedness methods we studied systematically a host of 18 ‘optimal’ graph search algorithms. In Chapter 3 of the thesis, we demonstrate, by extensively testing these algorithms on a variety of 3D medical images

Table 1: Average running time (in seconds) over 10 MRI scenes for fuzzy object tracking including affinity computation. Comparison of the cases of pre-computed affinities and on-the-fly computation for several objects.

how	what to compute	WM	GM	CSF
step-by-step	Affinity + Connectivity	22.12	23.87	25.60
	Affinity only	16.91	15.50	15.59
on-the-fly	Connectivity(+Affinity) whole	19.00	26.27	32.44
	Connectivity(+Affinity) with threshold	5.65	6.87	3.53

taken from large on-going applications, that substantial (700–35,500 fold) improvement over current speeds is achievable with a combination of well-chosen algorithms and fast modern PCs. These results were published in [14, 15].

3.1 Affinity Computation

Generally, in the fuzzy connectedness segmentation method, there are two major computational tasks: (i) computing the fuzzy affinity relations, and (ii) computing the fuzzy connectedness relations. Although affinity computation is straightforward, it has to be done separately for each object since the intensity features used for different objects may be different. This step was already optimized for speed by using integer arithmetics and lookup tables. However, if we know certain properties of the scenes and the objects in advance, we can minimize affinity computation by avoiding any computations for voxels that will definitely not be used during tracking. We discuss several strategies along these lines.

We tested two strategies for computing the fuzzy affinity relations: (S1) pre-compute affinities for all pairs of voxels having non-zero adjacency (i.e., neighboring voxels in our implementation) before tracking commences, and use as lookup tables during tracking, and (S2) compute affinities on-the-fly, when it is needed by the tracking algorithm for a certain pair of voxels (and store the computed values so that they can be reused by simple table lookup if referenced again).

(S1) is a good choice if the threshold for the fuzzy object is not known in advance and we want to experiment with different thresholds to find the optimum for the given fuzzy object. However, if a threshold is known in advance (e.g., the final threshold for the object, or the smallest from several thresholds to be used in case of the computation of fuzzy objects of different strengths), computing the affinity values for pairs of voxels that are not used in tracking is a waste of time, and so (S2) may be more efficient. Table 1 illustrates the difference between these two strategies.

3.2 Graph Search Algorithms

The computation of fuzzy connectedness values is accomplished via a graph search algorithm, which may be speeded up if efficient search strategies and data structures are used in the implementation. Most of the results presented in Chapter 3 address this efficiency problem.

Computing the fuzzy connectedness values for a fuzzy object is a variation of the single-source-shortest-path problem. This important graph theory problem and the associated algorithms are described in standard textbooks [1, 4]. We present two groups of algorithms in a general form so that the different variants, strategies and data structures used, all can be described in the same framework. These are modified versions of well-known algorithms for solving the single-source-shortest-path problem. Although there is no single “best” strategy (different strategies may be the “best” for different kinds of applications, and different affinity relations), we found a few variants that are good approximations to the (possibly) best in most cases.

The different data structures we utilized include: queue, priority queue, various heaps, LIFO and FIFO lists, hash tables with different hashing functions and table sizes. The strategies used are: different criteria for inserting a voxel in a queue, using different data structures to maintain the priority queue, using different hash functions (i.e., hashing by geometry-based properties or by affinity-based properties), and strategies for addressing the memory.

In the label-correcting family of algorithms, we implemented three different conditions in for inserting a voxel into the queue. We may use these conditions with or without an optional bit-array that keeps track of whether a voxel is already in the queue, in which case it need not be duplicated.

In one set of label-setting algorithms we represent the priority queue by a d -ary heap. The key of a voxel v in the queue is the tentative strength label $f_o(v)$ of v at the time it is inserted into the queue. In the first version of d -ary heap, we do not keep track of whether an element is already in the heap, and we do not perform a search in the heap for an already stored element, so we always insert a new instance of the voxel, even if it means duplication. In another version we maintain an additional pointer array, which, for every voxel v stores the position of v in the heap. The tracking algorithms in our final group using d -ary heaps are more memory-conserving. They use hash tables of various sizes with various hash functions to keep track of the positions of the voxels in the heap to make the the update operation efficient. We experimented with four hash functions and several sizes for the has table. One hash function was the commonly used linear addressing scheme of elements in multidimensional arrays, the others were simple ways of combining the three coordinates of a voxel into a single key value (+, *, XOR).

Fibonacci heap [4] is a novel data structure that allows the heap operations to be performed more efficiently than d -ary heaps. We used three versions of the tracking algorithm, analogous to those using d -ary heaps. With both types of heap structures, when hash tables are used to help the search for arbitrary elements in the heap, the hash function assigns the key value based on the coordinates of the voxel, which we may call hashing based on geometry.

Dial [5] gave a practical, very efficient implementation of Dijkstra’s shortest path algorithm. We modified his data structure and algorithm to compute fuzzy connectedness values. In our problem, since each voxel’s label (connectedness value) is bounded by the maximum possible affinity value, we can use the temporary connectedness strength label directly as a hashing key. We maintain a list of buckets, numbered $0, 1, \dots, A$, where A is the maximum possible (scaled integer) affinity value in the application, and each bucket k stores all nodes with the temporary connectedness value equal to k . When a voxel v is entered into the priority queue, its actual temporary label $f_o(v)$ is used as a hashing key, and v is put into the end of the corresponding bucket’s list. We tried two versions of the above described algorithm: with LIFO and FIFO version of bucket lists. We tested also a

Table 2: Average tracking time (in seconds) over 10 MRI scenes for different algorithms for different fuzzy objects using pre-computed affinities without using pre-determined thresholds for the objects (left) and with thresholds (right). Assignment of four-digit codes to individual algorithms are given in the thesis.

algorithm	WM	GM	CSF	algorithm	WM	GM	CSF
1023	35.47	71.82	109.48	0001	8.25	14.09	5.25
1021	30.71	61.15	90.19	0000	8.43	13.27	4.66
0000	22.19	48.28	70.05	0002	6.55	11.44	5.36
0001	19.35	38.89	53.23	0011	6.13	10.67	4.81
0002	15.40	29.97	40.84	0012	5.71	9.77	4.66
0011	14.33	27.63	35.29	0010	5.02	7.99	3.39
0010	13.18	27.42	36.42	1023	3.43	4.05	0.96
0012	13.20	25.11	32.24	1021	3.15	3.64	0.92
1022	5.94	10.46	16.51	1100	1.51	1.69	0.65
1201	5.98	7.92	18.52	1000	1.26	1.51	0.53
1120	5.95	9.27	12.42	1010	1.23	1.49	0.54
1020	5.48	8.69	11.70	1120	1.28	1.45	0.54
1100	5.60	8.20	10.36	1022	1.19	1.44	0.55
1010	4.94	7.12	9.02	1020	1.14	1.39	0.54
1000	4.64	7.00	8.56	1110	1.09	1.22	0.50
1110	4.46	6.19	8.11	1210	0.60	1.06	0.23
1210	2.56	4.17	4.93	1201	0.62	0.89	0.21
1200	2.17	2.95	6.15	1200	0.38	0.50	0.18

version, where an additional pointer array is used (as with the heaps) to make direct access of elements in the queue possible without searching through the bucket lists.

When the strength of object is specified in advance, the algorithms can make essential use of this information and terminate faster. Table 2 shows average tracking time for different algorithms for different fuzzy objects using pre-computed affinities with and without using pre-determined thresholds for the objects.

3.3 An MRI Protocol-independent Brain Segmentation Method

Despite the vast amount of literature and wide range of approaches to image segmentation, general, reusable frameworks seem to be lacking. General frameworks, that are readily applicable to images acquired with different protocols do not seem to have been published. Most papers deal with methods devised for specific tasks, tailored to a specific acquisition protocol and body region. In many cases, the segmentation method is a simple, *ad hoc* combination of basic tools or some more sophisticated combination involving heavy “engineering”. What we need is a segmentation “workshop” wherein a protocol-specific segmentation method can be quickly fabricated. That is, for a new protocol, the workshop allows quick experimentation to complete the set up phase quickly rather than requiring months and years of basic research and development.

We devised one such workshop for brain MRI segmentation and present it in Chapter 4

of the thesis. The method (published in [23]) combines the robust, accurate, and efficient techniques of fuzzy connectedness segmentation with standardized MRI intensities [19, 26] (see Chapter 2 of the thesis) and fast algorithms [14] (see Chapter 3 of the thesis). The result is a general segmentation framework that efficiently utilizes the user input (for recognition) and the power of computer (for delineation). This same two-phase method has been applied to segment brain tissues from a variety of MRI protocols.

The method we devised using the general framework is an approach to the segmentation of the whole brain parenchyma (BP), as well as to the precise quantification of gray matter (GM) and white matter (WM) on several routinely acquired MR images of MS patients, such as fast spin-echo (FSE) proton density (PD) and T2-weighted, T1-weighted, and spoiled-gradient (SPGR) images. First, the segmentation procedure is set up, parameters are trained for, and fine tuned. This is performed only once for each protocol. Then, each dataset is segmented into the desired objects (i.e., BP, WM and GM). Figure 2 shows scenes representing the standardized FSE PD, T2 study pair, the fuzzy affinity relations, the connectedness values, and the hard segmentation for the GM, WM, and CSF objects. The main steps of the segmentation method are the followings.

TS1-TS5: Training and set up.

SS1: Correct for RF field inhomogeneity by using a completely automatic method that is acquisition-protocol-independent, and requires no prior knowledge [36].

SS2: Standardize the MR image intensities using the method described in Chapter 2 of the thesis.

SS3: Compute fuzzy affinity using scale-based features [31].

SS4: Specify volume of interest and seed points for each of WM, GM, and ventricular CSF.

SS5: Compute relative fuzzy connectedness [29] to determine the fuzzy objects for different tissues.

SS6: Create the brain mask by combining GM, WM, and CSF masks and then applying some morphological operators to fill holes and reduce misclassification error.

SS7: Verification and correction (if necessary) of the brain mask is performed by the operator. These corrections are mainly removing extracranial regions that may get connected to the brain via weak links of fuzzy connectedness.

SS8: Create masks for each object by recalculating GM and WM objects within the corrected brain mask.

SS9: Compute volume by simply multiplying the number of voxels within the object's binary mask by the voxel volume.

Most steps are automatic, their parameters are determined and fixed in the training and setup phase. Depending on what acquisition protocol was used, small differences may be present as to how fuzzy affinity is computed.

For the training phase, for each protocol, a few datasets are selected and used to extract the values for the parameters. The training procedure mostly requires continuous user control, since the fine tuning of parameters is a modify-and-verify iteration. The major steps of the training phase are the followings.

TS1: Perform the initial steps of the segmentation algorithm (SS1-SS2). In this phase, SS4 (seed and VOI specification) may also be performed in advance.

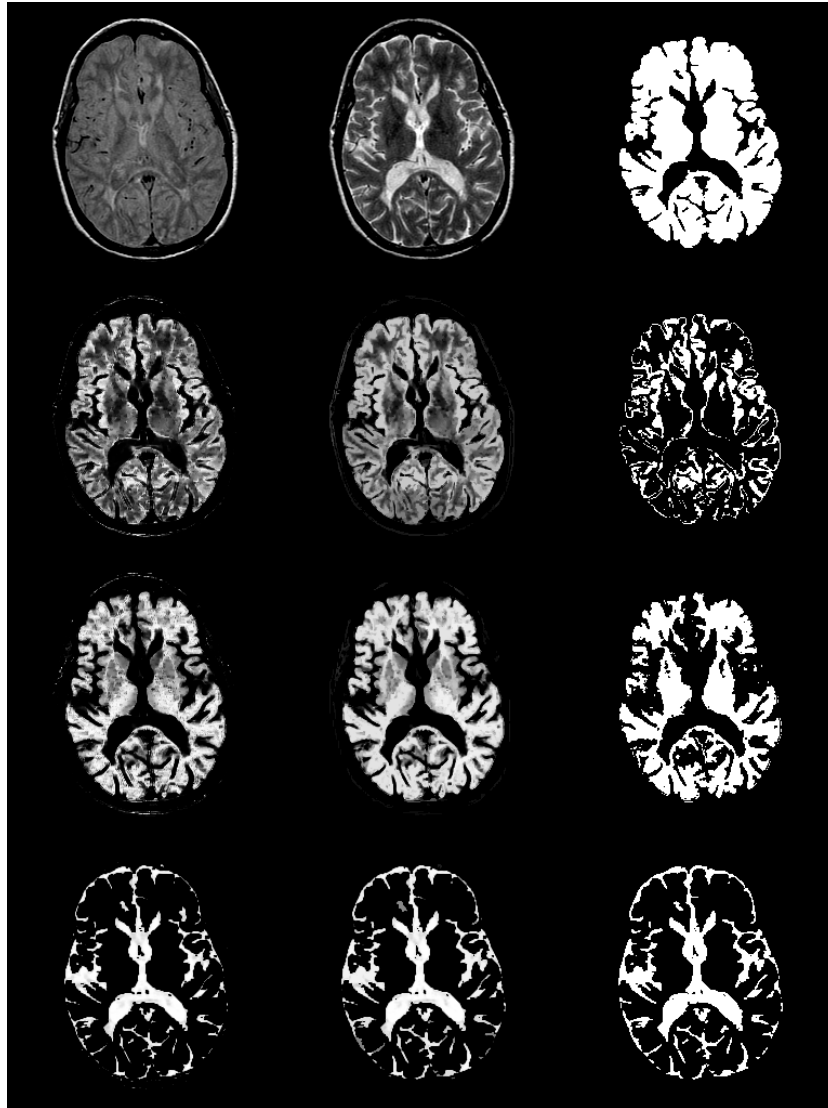


Figure 2: Slices from a standardized FSE PD, T2 study pair (top row, left and middle images), the corresponding slices from the scenes depicting the fuzzy affinity relations for the GM, WM, and CSF objects (first column), the same slices from the scenes depicting the connectedness values (second column), and the hard (binary) segmented objects (third column). Binary mask for brain parenchyma is shown in the top right image.

TS2: Determine threshold intervals to roughly segment the different tissues (CSF, WM, GM) in the intensity images. From the parameters of the distribution of intensities within these segmented regions compute initial values for setting up the fuzzy affinity relations.

TS3: Perform the segmentation steps of the algorithm (SS3-SS8).

TS4: Evaluate the segmented objects and, if necessary, modify the parameters and go to TS3.

TS5: Save the found best parameters for future use.

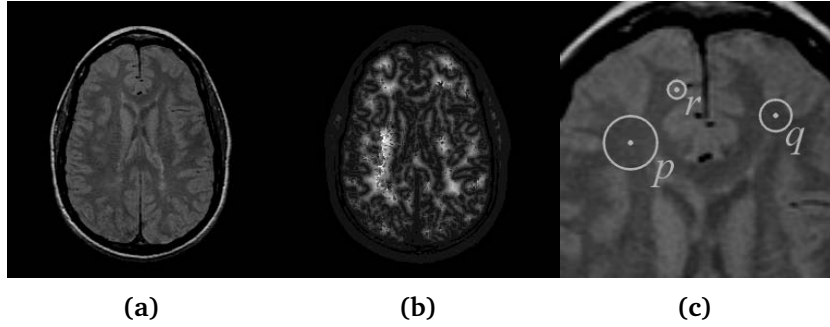


Figure 3: Illustration of local structure size (scale). An MRI slice of a MS patient’s head (a), the corresponding scale image (b), and part of the original slice enlarged (c) to show details. In (b), scale values are not shown for the background part of the slice.

4 Image Registration

To be able to utilize the complementary information from multiprotocol acquisitions, or for longitudinal image analysis, the images need to be in spatial correspondence. Image registration is used to achieve this correspondence. Intra-subject image registration is used for matching multiple acquisitions for the same study or for matching longitudinal acquisitions. Inter-subject registration is used when creating atlases (of “average” anatomy), or when using the atlases in individual cases (e.g., for matching the atlas to the study in question and classifying the tissues based on the pre-determined classification of the atlas).

In Chapter 5 of the thesis, we present a new class of approaches for rigid-body registration. We compare their performance with several commonly used strategies in studying Multiple Sclerosis via multi protocol MRI. The approach and the comparison results were published in [24, 25].

4.1 Scale as a New Feature

In scene-based methods, the match/mismatch criterion function may be computed directly from the input scenes or from some feature scenes extracted from the original values. Several features (such as edges, ridges, troughs), have been proposed for scene-based image registration in the past [12]. We propose a new feature—the (local) object-scale—that has been recently used for aiding image segmentation [31] and filtering [30].

“Scale” is a fundamental, well-established concept in image processing [10]. Our idea of “scale” [31], which is somewhat different from a similar concept used in computer vision [10], is to determine the size of local structures under a prespecified region-homogeneity criterion. For example, in Fig. 3, local size of the structure to which voxel p belongs is bigger than that to which q or r belongs. The scale image for the MR slice of an MS patient’s head, shown in Fig. 3 (a), is shown in Fig. 3 (b). The image shows that interior regions have higher scale (brighter intensities) while detailed structured regions as well as boundary vicinities have lower scale (darker intensities).

One set of our new methods used scale values directly as registration feature. In these cases, the registration method tries to match potential boundary regions to boundary regions, and homogeneous “flat” regions to flat regions. Incorporating boundary information in this manner into the registration method results in improved matching accuracy in certain cases. Our approach has the advantage of not requiring edge detection or explicit segmenta-

tion (which is a challenging task on its own). It uses information relating to the approximate whereabouts of the boundaries (regions of small scale) in a fuzzy manner.

4.2 The Studied Registration Methods

In our application (registering MRI head datasets for the purpose of computing MS disease-specific measures), the rigid-body assumption (i.e., the two scenes can be matched by global translations and rotations only) is satisfied well. The geometric part of a 3D rigid-body transformation can be described by six parameters: three global translation components and three rotation angles around the three coordinate axes. For the interpolation part, we used trilinear interpolation.

There are several measures proposed in the literature to define the degree of mismatch of two scenes. We utilized three different matching criteria to guide the search for optimum registration: cross-correlation, normalized cross-correlation and mutual information. Having these three criteria and letting the scenes be also scale images of the given reference and test scenes, we consider the following six strategies for registration: correlation of original scenes (c,o), correlation of scale scenes (c,s), normalized correlation of original scenes (cn,o), normalized correlation of scale scenes (cn,s), mutual information in original scenes (m,o), and mutual information in scale scenes (m,s).

To reduce computation but still have the necessary capture range and precision, we used a multi-level approach. Multi-level methods are widely used in the literature for registration [11, 27, 32]. They have proved effective in reducing computation time as well as in helping to avoid local minima. In this study, we used a three-level Gaussian pyramid. At each hierarchy level, an optimal solution was determined which was used as the starting point for the next level. At the lowest resolution, the transformation was initialized by the principal axes method. Powell’s multidimensional direction set method [28] was used to optimize the mismatch function by using Brent’s one-dimensional optimization algorithm for line minimizations.

4.3 Methods of Comparison

We assessed *intra-modality accuracy* for each protocol in the set {PD, T2, T1, T1E, MT1, MT2}, for each method of {(c,o), (cn,o), (m,o), (c,s), (cn,s), (m,s)}. Using the pairs (PD, T2) and (MT1, MT2) which were in registration at acquisition, we assessed *inter-modality accuracy* in a similar way. *Inter-modality consistency* can also be assessed by utilizing the registered pairs. For each test we take a scene and reslice it to create an artificially misregistered version by applying a known transformation. The registration algorithm is then applied to find the transformation which registers the misregistered version to the original. In each experiment, we compare two transformations. In the *accuracy* tests, these are the known misregistration and the transformation found by the method in case, and they are expected to be the inverse of each other. In the *consistency* tests, the two registrations to scenes of the registered pair are compared and they are expected to be equal.

We devised a ranking system for the methods as follows. Each registration task is performed on datasets of 10 patients. For each method and misregistration (and patient data), for each comparison, we computed the mean of the RMS error for the 8 corner voxels of the box approximately bounding the head. We can use the paired t-test to compare the errors of two methods performing the same task (same misregistration, same protocol, 10 differ-

Table 3: Comparison of methods for intra-, inter-protocol registration and for consistency, for different misregistrations.

	method	small	medium	large	total
intra-protocol	(c,o)	2.188	0.192	0.046	0.344
	(cn,o)	1.991	0.117	21.625	1.550
	(m,o)	3.222	421.000	6.250	10.346
	(c,s)	0.353	1.230	0.457	0.580
	(cn,s)	0.192	1.230	0.675	0.568
	(m,s)	0.707	1.000	0.812	0.831
inter-protocol	(c,o)	1.355	1.176	1.000	1.168
	(cn,o)	0.400	0.615	4.281	0.940
	(m,o)	1.153	0.737	0.867	0.907
	(c,s)	1.413	1.153	0.737	1.053
	(cn,s)	1.000	1.153	0.615	0.907
	(m,s)	1.000	1.355	0.867	1.050
consistency	(c,o)	2.828	1.153	1.286	1.555
	(cn,o)	0.502	0.928	1.991	0.972
	(m,o)	1.071	0.933	0.737	0.909
	(c,s)	1.679	1.071	0.737	1.080
	(cn,s)	0.557	0.801	0.801	0.717
	(m,s)	0.801	1.153	1.000	0.976

ent datasets). Based on the mean RMS error, one of the two methods is either significantly better than the other (i.e., smaller error), or there is no significant difference between the two in performing that particular task. For each misregistration group, for each reasonable pair of methods, for each task (protocol, accuracy/consistency test), we count the number of occurrences of significant wins, losses, and nonsignificant differences of the methods in question. Based on a combination of these counts, we rank the methods within a particular task. Table 3 contains these ranks for intra- and inter-protocol registration tasks and for consistency of the different methods for small, medium, and large misalignment cases.

5 Image Analysis in Multiple Sclerosis

Multiple Sclerosis (MS) is an acquired disease of the central nervous system. Since its first description in 1877, it has been investigated extensively. In its advanced state, the disease may severely impair the ambulatory ability and may even cause death. There are several clinical measures commonly used to express the severity of the disease. These measures are subjective and may have reproducibility problems. The development of new treatments demands objective outcome measures for relatively short trials. MR imaging has proven to be a very sensitive marker of the MS disease. A variety of protocols are being investigated for improving the conspicuity of the lesions in the images in the early stage and in the advanced stage for both the microscopic and macroscopic processes.

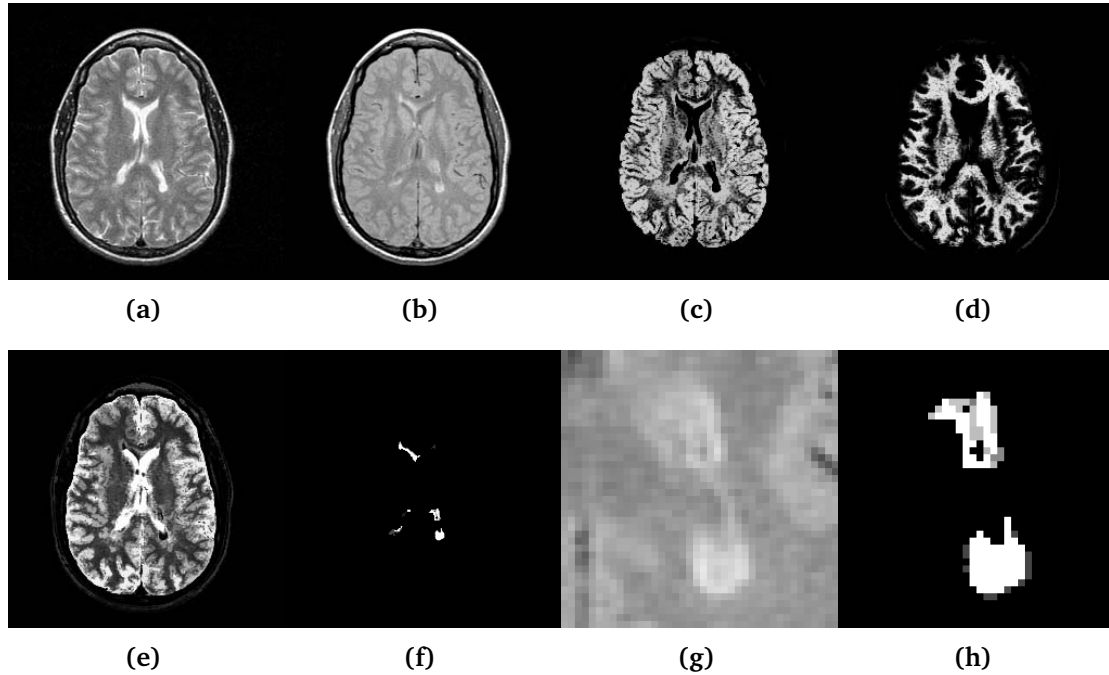


Figure 4: T2 (a) and PD (b) images of a MS patient. The GM (c), WM (d), CSF (e), and lesion (f) objects segmented as 3D fuzzy connected objects are shown in the slices. A close up of one of the lesions (g) and its fuzzy segmentation (h) are also shown to emphasize the fuzzy nature of the lesion.

In an attempt to eventually replace Expanded Disability Status Scale (EDSS)—a widely used but rather subjective measure—by an objective measure to assess the natural course of the disease and its response to therapy, we have developed image segmentation methods based on fuzzy connectedness to quantify various objects in multiprotocol MRI. Figure 4 illustrates the output of the method.

A review of MR image analysis techniques currently used in MS is given in Chapter 6 of the thesis. Also, the family of techniques using fuzzy connectedness for different protocols is described and evaluated. The content of this chapter was published in [20, 33, 34].

6 Contributions of the Thesis

Contributions in the first group are described in Chapter 2 and were published in journal articles [19, 26] and proceedings papers [17, 18, 22].

- 1/1. We developed an image processing method (algorithms and theory for correctness) for MRI intensity standardization wherein all images can be transformed in such a way that for the same protocol and body region, in the transformed images similar intensities will have similar tissue meaning.
- 1/2. We showed through image display examples that the consistency of the brightness level and contrast of images is considerably improved after standardization and showed that the tissues have much more consistent intensity ranges if the new variants of the standardizing method are used. We demonstrated, in quantitative studies, that the scanner dependent intra- and inter-patient intensity variations are substantially reduced after standardization.

Contributions in the second group are described in Chapter 3 and were published in the journal article [14] and proceedings paper [15].

- 2/1. We studied systematically a host of 18 ‘optimal’ graph search algorithms and demonstrated, by extensively testing these algorithms on a variety of 3D medical images taken from large on-going applications, that substantial improvement in speeding up the fuzzy connectedness methods is achievable with a combination of well-chosen algorithms and fast modern PCs.
- 2/2. We showed that utilizing efficient algorithms and careful selection of implementations can speed up the computation of fuzzy connectedness values by a factor of 16 to 29 (on the same hardware), as compared to the implementation previously used in applications utilizing fuzzy object segmentation.
- 2/3. We found that the label-setting algorithms are faster than the label-correcting algorithms in real applications, as the theoretical complexity analysis suggested. However, those using more complicated data structures are not the fastest in practice. We suggested a general guideline for selecting an algorithm depending on the structure of objects to be segmented and their intensity distribution.

Contribution in the third group is described in Chapter 4 and was published in the proceedings paper [23].

3. Using the fast algorithms proposed herein on fast hardware, interactive speed of fuzzy object segmentation is achievable. This leads to a new line of segmentation techniques. If images having intensities with tissue-specific meaning (such as standardized MR images) are utilized, most of the parameters for the segmentation method can be fixed once for all, all intermediate data can be computed before the user interaction is needed and the user can be provided with more information at the time of interaction. The reliable recognition (assisted by human operators) and the accurate, efficient, and sophisticated delineation (automatically performed by the computer) can be effectively incorporated into a single interactive process.

Contributions in the fourth group are described in Chapter 5 and were published in the journal article [24] and proceedings paper [25].

- 4/1. We presented a new class of approaches, using local scale information, for rigid-body image registration. We compared the performance of the new scale-based registration methods with several commonly used strategies in studying Multiple Sclerosis via multi protocol MRI. We devised and used a new ranking system for the comparison of the registration methods.
- 4/2. We analyzed both intra- and inter-protocol registration results among the methods for 3D data of the head, acquired from 10 MS patients using 6 MRI protocols. Our analysis indicates that there is no “best” method, although there are significant differences in the performance of the methods, for the particular application of combining information from multiprotocol MR imagery for studying MS.

Contribution in the fifth group is described in Chapter 6 and was published in the book chapter [20], the journal article [34], and proceedings paper [33].

5. We reviewed MR image analysis techniques currently used in MS and we described and evaluated the family of techniques using fuzzy connectedness for different protocols.

References

- [1] R. K. Ahuja, T. L. Magnanti, and J. B. Orlin. *Network Flows : Theory, Algorithms, and Applications*, chapters 4, 5, A. Prentice-Hall, Englewood Cliffs, NJ, February 1993.
- [2] I. Catalaa, R. I. Grossman, D. L. Kolson, L. G. Nyúl, L. Wei, J. K. Udupa, M. Polansky, and J. C. McGowan. Magnetization transfer histogram analysis of segmented normal-appearing white matter in multiple sclerosis. In *ISMRM Seventh Meeting Proceedings, 22-28 May 1999, Philadelphia, PA*, page 957, May 1999.
- [3] I. Catalaa, R. I. Grossman, D. L. Kolson, J. K. Udupa, L. G. Nyúl, L. Wei, X. Zhang, M. Polansky, L. J. Mannon, and J. C. McGowan. Multiple sclerosis: Magnetization transfer histogram analysis of segmented normal-appearing white matter. *Radiology*, 216(2):351–355, August 2000.
- [4] T. H. Cormen, C. E. Leiserson, and R. L. Rivest. *Introduction to Algorithms*, chapters 7, 12, 16, 20, 21, 25. The MIT Press, Cambridge, MA, June 1990.
- [5] R. B. Dial. Algorithm 360: Shortest-path forest with topological ordering. *Communications of the ACM*, 12(11):632–633, November 1969.
- [6] Y. Ge, R. I. Grossman, J. K. Udupa, J. S. Babb, L. G. Nyúl, and D. L. Kolson. Brain atrophy in relapsing-remitting multiple sclerosis: Fractional volumetric analysis of gray matter and white matter. *Radiology*, 220(3):606–610, September 2001.
- [7] Y. Ge, R. I. Grossman, J. K. Udupa, J. S. Babb, L. G. Nyúl, and J. C. McGowan. Tissue characterization in relapsing-remitting and secondary-progressive MS via magnetization transfer ratio. In *ISMRM Eighth Meeting Proceedings, 1-7 April 2000, Denver, CO*, volume 2, page 1189, April 2000.
- [8] Y. Ge, J. K. Udupa, L. G. Nyúl, L. Wei, and R. I. Grossman. Numerical tissue characterization in MS via standardization of the MR image intensity scale. *Journal of Magnetic Resonance Imaging*, 12(5):715–721, November 2000.
- [9] Y. Ge, J. K. Udupa, L. G. Nyúl, L. Wei, and R. I. Grossman. Numerical tissue characterization in MS via standardization of the MR image intensity scale. In *ISMRM Eighth Meeting Proceedings, 1-7 April 2000, Denver, CO*, volume 1, page 579, April 2000.
- [10] T. Lindeberg. *Scale-space Theory in Computer Vision*, volume 256 of *The Kluwer International Series in Engineering and Computer Science*. Kluwer Academic Publishers, Boston, MA, December 1993.
- [11] F. Maes, D. Vandermeulen, and P. Suetens. Comparative evaluation of multiresolution optimization strategies for multimodality image registration by maximization of mutual information. *Medical Image Analysis*, 3(4):373–386, December 1999.
- [12] J. B. A. Maintz, P. A. van den Elsen, and M. A. Viergever. Comparison of edge-based and ridge-based registration of CT and MR brain images. *Medical Image Analysis*, 1(2): 151–161, June 1996.

- [13] L. Nyúl and J. K. Udupa. Többdimenziós MRI képek feldolgozása. In A. Kuba, E. Máté, and K. Palágyi, editors, *Book of Abstracts, KEPAF 2002, Domaszék, Hungary, 23-25 January, 2002*, pages 96–97, January 2002.
- [14] L. G. Nyúl, A. X. Falcão, and J. K. Udupa. Fuzzy-connected 3D object segmentation at interactive speeds. *Graphical Models*, 1999. submitted for publication.
- [15] L. G. Nyúl, A. X. Falcão, and J. K. Udupa. Fuzzy-connected 3D image segmentation at interactive speeds. In K. M. Hanson, editor, *Medical Imaging 2000: Image Processing*, volume 3979 of *Proceedings of SPIE*, pages 212–223, June 2000.
- [16] L. G. Nyúl and J. K. Udupa. On standardizing the MR image intensity scale. *Radiology*, 209(P):581–582, November 1998.
- [17] L. G. Nyúl and J. K. Udupa. An approach to standardizing the MR image intensity scale. In S. K. Mun and Y. Kim, editors, *Medical Imaging 1999: Image Display*, volume 3658 of *Proceedings of SPIE*, pages 595–603, May 1999.
- [18] L. G. Nyúl and J. K. Udupa. New variants of a method of MRI scale normalization. In A. Kuba, M. Šámal, and A. Todd-Pokropek, editors, *Information Processing in Medical Imaging: 16th International Conference, IPMI'99, Proceedings*, volume 1613 of *Lecture Notes on Computer Science*, pages 490–495, Berlin, June–July 1999.
- [19] L. G. Nyúl and J. K. Udupa. On standardizing the MR image intensity scale. *Magnetic Resonance in Medicine*, 42(6):1072–1081, December 1999.
- [20] L. G. Nyúl and J. K. Udupa. MR image analysis in multiple sclerosis. In J. A. Frank, editor, *Advances in Multiple Sclerosis*, volume 10(4) of *Neuroimaging Clinics of North America*, pages 799–816. W. B. Saunders Company, Philadelphia, PA, November 2000.
- [21] L. G. Nyúl and J. K. Udupa. Standardizing the MR image intensity scale and its applications. In T. Csendes, editor, *Book of Abstracts, Conference of PhD Students in Computer Science, July 20-23, 2000, Szeged, Hungary*, page 75, July 2000.
- [22] L. G. Nyúl and J. K. Udupa. Standardizing the MR image intensity scales: Making MR intensities have tissue-specific meaning. In S. K. Mun, editor, *Medical Imaging 2000: Image Display*, volume 3976 of *Proceedings of SPIE*, pages 496–504, April 2000.
- [23] L. G. Nyúl and J. K. Udupa. A protocol-independent brain MRI segmentation method. In M. Sonka and J. M. Fitzpatrick, editors, *Medical Imaging 2002: Image Processing*, volume 4684 of *Proceedings of SPIE*, pages 1588–1599, May 2002.
- [24] L. G. Nyúl, J. K. Udupa, and P. K. Saha. Task-specific comparison of 3-D image registration methods. *IEEE Transactions on Medical Imaging*, 2001. submitted for publication.
- [25] L. G. Nyúl, J. K. Udupa, and P. K. Saha. Task-specific comparison of 3-D image registration methods. In M. Sonka and K. M. Hanson, editors, *Medical Imaging 2001: Image Processing*, volume 4322 of *Proceedings of SPIE*, pages 1588–1598, July 2001.
- [26] L. G. Nyúl, J. K. Udupa, and X. Zhang. New variants of a method of MRI scale standardization. *IEEE Transactions on Medical Imaging*, 19(2):143–150, February 2000.

- [27] K. Palágyi and J. K. Udupa. Medical image registration based on fuzzy objects. In *Proceedings of the 3rd Workshop on Computational Modelling, Imaging and Visualization in Biosciences, COMBIO'96, Sopron, Hungary, 29-31 August 1996*, pages 44–48, 1996.
- [28] W. H. Press, S. A. Teukolsky, W. T. Vetterling, and B. P. Flannery. *Numerical Recipes in C: The Art of Scientific Computing*. Cambridge University Press, Cambridge, 2nd edition, 1992.
- [29] P. K. Saha and J. K. Udupa. Relative fuzzy connectedness among multiple objects: Theory, algorithms, and applications in image segmentation. *Computer Vision and Image Understanding : CVIU*, 82(1):42–56, April 2001.
- [30] P. K. Saha and J. K. Udupa. Scale-based diffusive image filtering preserving boundary sharpness and fine structures. *IEEE Transactions on Medical Imaging*, 20(11):1140–1155, November 2001.
- [31] P. K. Saha, J. K. Udupa, and D. Odhner. Scale-based fuzzy connected image segmentation: Theory, algorithms, and validation. *Computer Vision and Image Understanding : CVIU*, 77(2):145–174, February 1999.
- [32] C. Studholme, D. L. G. Hill, and D. J. Hawkes. Automated three-dimensional registration of magnetic resonance and positron emission tomography brain images by multiresolution optimization of voxel similarity measures. *Medical Physics*, 24(1):25–35, January 1997.
- [33] J. K. Udupa, L. G. Nyúl, Y. Ge, and R. I. Grossman. Multiprotocol MR image segmentation in multiple sclerosis: Experience with over 1000 studies. In K. M. Hanson, editor, *Medical Imaging 2000: Image Processing*, volume 3979 of *Proceedings of SPIE*, pages 1017–1027, June 2000.
- [34] J. K. Udupa, L. G. Nyúl, Y. Ge, and R. I. Grossman. Multiprotocol MR image segmentation in multiple sclerosis: Experience with over 1000 studies. *Academic Radiology*, 8(11):1116–1126, November 2001.
- [35] J. K. Udupa and S. Samarasekera. Fuzzy connectedness and object definition: Theory, algorithms, and applications in image segmentation. *Graphical Models and Image Processing*, 58(3):246–261, May 1996.
- [36] Y. Zhuge, J. K. Udupa, J. Liu, P. K. Saha, and T. Iwanaga. Scale-based method for correcting background intensity variation in acquired images. In M. Sonka and M. J. Fitzpatrick, editors, *Medical Imaging 2002: Image Processing*, volume 4684 of *Proceedings of SPIE*, pages 1103–1111, May 2002.

The author's publications on the subjects of the thesis

Chapters in books

L. G. Nyúl and J. K. Udupa. MR image analysis in multiple sclerosis. In J. A. Frank, editor, *Advances in Multiple Sclerosis*, volume 10(4) of *Neuroimaging Clinics of North America*, pages 799–816. W. B. Saunders Company, Philadelphia, PA, November 2000.

Articles in peer reviewed journals

I. Catalaa, R. I. Grossman, D. L. Kolson, J. K. Udupa, L. G. Nyúl, L. Wei, X. Zhang, M. Polansky, L. J. Mannon, and J. C. McGowan. Multiple sclerosis: Magnetization transfer histogram analysis of segmented normal-appearing white matter. *Radiology*, 216(2):351–355, August 2000.

Y. Ge, R. I. Grossman, J. K. Udupa, J. S. Babb, L. G. Nyúl, and D. L. Kolson. Brain atrophy in relapsing-remitting multiple sclerosis: Fractional volumetric analysis of gray matter and white matter. *Radiology*, 220(3):606–610, September 2001.

Y. Ge, J. K. Udupa, L. G. Nyúl, L. Wei, and R. I. Grossman. Numerical tissue characterization in MS via standardization of the MR image intensity scale. *Journal of Magnetic Resonance Imaging*, 12(5):715–721, November 2000.

L. G. Nyúl, A. X. Falcão, and J. K. Udupa. Fuzzy-connected 3D object segmentation at interactive speeds. *Graphical Models*, 1999. submitted for publication.

L. G. Nyúl and J. K. Udupa. On standardizing the MR image intensity scale. *Magnetic Resonance in Medicine*, 42(6):1072–1081, December 1999.

L. G. Nyúl, J. K. Udupa, and P. K. Saha. Task-specific comparison of 3-D image registration methods. *IEEE Transactions on Medical Imaging*, 2001. submitted for publication.

L. G. Nyúl, J. K. Udupa, and X. Zhang. New variants of a method of MRI scale standardization. *IEEE Transactions on Medical Imaging*, 19(2):143–150, February 2000.

J. K. Udupa, L. G. Nyúl, Y. Ge, and R. I. Grossman. Multiprotocol MR image segmentation in multiple sclerosis: Experience with over 1000 studies. *Academic Radiology*, 8(11):1116–1126, November 2001.

Full papers in conference proceedings

L. G. Nyúl, A. X. Falcão, and J. K. Udupa. Fuzzy-connected 3D image segmentation at interactive speeds. In K. M. Hanson, editor, *Medical Imaging 2000: Image Processing*, volume 3979 of *Proceedings of SPIE*, pages 212–223, June 2000.

L. G. Nyúl and J. K. Udupa. An approach to standardizing the MR image intensity scale. In S. K. Mun and Y. Kim, editors, *Medical Imaging 1999: Image Display*, volume 3658 of *Proceedings of SPIE*, pages 595–603, May 1999.

L. G. Nyúl and J. K. Udupa. New variants of a method of MRI scale normalization. In A. Kuba, M. Šámal, and A. Todd-Pokropek, editors, *Information Processing in Medical Imaging: 16th International Conference, IPMI'99, Proceedings*, volume 1613 of *Lecture Notes on Computer Science*, pages 490–495, Berlin, June–July 1999.

L. G. Nyúl and J. K. Udupa. Standardizing the MR image intensity scales: Making MR intensities have tissue-specific meaning. In S. K. Mun, editor, *Medical Imaging 2000: Image Display*, volume 3976 of *Proceedings of SPIE*, pages 496–504, April 2000.

L. G. Nyúl and J. K. Udupa. A protocol-independent brain MRI segmentation method. In M. Sonka and J. M. Fitzpatrick, editors, *Medical Imaging 2002: Image Processing*, volume 4684 of *Proceedings of SPIE*, pages 1588–1599, May 2002.

L. G. Nyúl, J. K. Udupa, and P. K. Saha. Task-specific comparison of 3-D image registration methods. In M. Sonka and K. M. Hanson, editors, *Medical Imaging 2001: Image Processing*, volume 4322 of *Proceedings of SPIE*, pages 1588–1598, July 2001.

J. K. Udupa, L. G. Nyúl, Y. Ge, and R. I. Grossman. Multiprotocol MR image segmentation in multiple sclerosis: Experience with over 1000 studies. In K. M. Hanson, editor, *Medical Imaging 2000: Image Processing*, volume 3979 of *Proceedings of SPIE*, pages 1017–1027, June 2000.

Conference abstracts and extended abstracts

I. Catalaa, R. I. Grossman, D. L. Kolson, L. G. Nyúl, L. Wei, J. K. Udupa, M. Polansky, and J. C. McGowan. Magnetization transfer histogram analysis of segmented normal-appearing white matter in multiple sclerosis. In *ISMRM Seventh Meeting Proceedings, 22-28 May 1999, Philadelphia, PA*, page 957, May 1999.

Y. Ge, J. K. Udupa, L. G. Nyúl, L. Wei, and R. I. Grossman. Numerical tissue characterization in MS via standardization of the MR image intensity scale. In *ISMRM Eighth Meeting Proceedings, 1-7 April 2000, Denver, CO*, volume 1, page 579, April 2000.

Y. Ge, R. I. Grossman, J. K. Udupa, J. S. Babb, L. G. Nyúl, and J. C. McGowan. Tissue characterization in relapsing-remitting and secondary-progressive MS via magnetization transfer ratio. In *ISMRM Eighth Meeting Proceedings, 1-7 April 2000, Denver, CO*, volume 2, page 1189, April 2000.

L. Nyúl and J. K. Udupa. Többdimenziós MRI képek feldolgozása. In A. Kuba, E. Máté, and K. Palágyi, editors, *Book of Abstracts, KEPAF 2002, Domaszék, Hungary, 23-25 January, 2002*, pages 96–97, January 2002.

L. G. Nyúl and J. K. Udupa. On standardizing the MR image intensity scale. *Radiology*, 209 (P):581–582, November 1998.

L. G. Nyúl and J. K. Udupa. Standardizing the MR image intensity scale and its applications. In T. Csendes, editor, *Book of Abstracts, Conference of PhD Students in Computer Science, July 20-23, 2000, Szeged, Hungary*, page 75, July 2000.

